# Structural Relaxation of Ultrathin Polymer Films Prepared by the Langmuir−Blodgett Technique: Characteristics of the Two-Dimensional System

**Michiaki Mabuchi,[†] Kenji Kawano,[†] Shinzaburo Ito,[†] Masahide Yamamoto,*[,†] Masaoki Takahashi,[‡] and Toshiro Masuda[‡]**

*Departments of Polymer Chemistry and Material Chemistry, Graduate School of Engineering, Kyoto University, Yoshida, Sakyo, Kyoto 606-8501, Japan*

*Received March 3, 1998; Revised Manuscript Received June 7, 1998*

ABSTRACT: Thermal relaxation of ultrathin polymer films prepared by the Langmuir−Blodgett (LB) technique was studied by a comparison with a three-dimesional bulk system. Poly(vinyl alkanal acetal)s (PVAA) with different side chain lengths were synthesized and the thermal stability of their LB films was investigated by the energy-transfer phenomenon between fluorescence probes labeled to the polymer chains. The multilayer structure was irreversibly disordered and mixed by the thermal treatment. A close relationship was found between the glass-transition temperature ($T_g$) of the polymer bulk and the temperature at which the layered structure of LB films started to disorder. Theoretical calculations based on Förster kinetics were applied to measure the diffusivity of polymer segments, which was successfully evaluated by assuming time-dependent Gaussian distributions of chromophores in the direction normal to the layer plane. The apparent activation energy $\Delta E_a$ of the diffusion constant for the LB films, however, was much smaller than that for polymer bulk obtained by the viscoelastic measurement. It was concluded that the relaxation process of the ultrathin polymer films occurs by conformational changes from the two-dimensional nonequilibrium state given by the LB deposition. The confined form could be released by the local motion of the polymer segments under the heating to temperatures higher than $T_g$.

## Introduction

The LB technique is one of many fascinating methods to fabricate artificial molecular assemblies of organic materials in mild conditions.[1] Since Kuhn et al. showed that fundamental photochemical and photophysical processes such as energy transfer and electron transfer can be controlled by the layer structure,[2] extensive investigations on LB films have been made to design and fabricate molecular devices. For the application of LB films, the thermal stability of layered structure after the deposition is an issue of both fundamental and practical importance. Conventional fatty acid films have low thermal and mechanical stability and their as-deposited structure is disordered during the first few days or weeks. One approach to improve the thermal stability is the use of polymers.[3] Expected to overcome such drawbacks of low-molecular LB films, many kinds of polymers have been designed, synthesized, and developed for the LB materials. Most of them are polymers having a flexible main chain. Poly(vinyl alkanal acetal) (PVAA) is a representative of these polymers with high transferability in the wide range of the conditions.[4] Besides, PVAA is also useful as a base polymer to which various kinds of functional moieties can be introduced as a side chain.[5]

To examine thermal stability of polymer LB films, small-angle X-ray scattering[6,7] is used to probe the periodic layered structure, and polarized infrared spectroscopy[8,9] and optical second-harmonic generation (SHG) method[10] to probe the orientational stability of polymer side chains. We employed the energy-transfer technique to study the structural relaxation of the polymer LB films in nanometer dimensions.[11−16] It is powerful to observe the microscopic change in the ultrathin films because of high sensitivity. Particularly, in amorphous polymer LB films, which do not show clear peaks of X-ray reflection due to their low contrast of electron density, the energy-transfer method is effective for structural analysis. Previously, we reported that the multilayer structure of LB films is irreversibly disordered to a stable equilibrium state by heating. Because LB films have a multilayer structure in which each layer is in a quasi two-dimensional (2D) array, some characteristic properties due to the polymer conformation are expected during the process of thermal relaxation. Here, we studied thermal relaxation of PVAA multilayers by the energy-transfer method and characterized their thermal properties in terms of relaxation temperature and activation energy for the diffusion coefficients, in comparison with the those of the three-dimensional (3D) polymer bulk.

## Experimental Section

**Materials.** PVAAs (Chart 1) were synthesized by acetalization of commercial poly(vinyl alcohol) (PVA, Wako Pure Chemical Industries; degree of polymerization = 2000). Details have been described elsewhere.[10] The polymer was labeled with phenanthrene (P) or anthracene (A) chromophores by the reaction with the corresponding chromophoric aldehyde (Aldrich).

Table 1 shows the percentages of alkyl units and chromophoric units in the acetalized polymers, poly(vinyl butanal acetal) (PVB), poly(vinyl pentanal acetal) (PVP), and poly(vinyl octanal acetal) (PVO), where butanal, pentanal, and octanal were employed as the alkyl group, respectively. These percentages were determined by UV absorption of the phenanthrene unit (the extinction coefficient is 11 750 L mol$^{-1}$ cm$^{-1}$ at 298 nm) and the anthracene unit (8800 L mol$^{-1}$ cm$^{-1}$ at 364 nm), and from the carbon fraction measured by elementary analysis. For the energy-transfer measurement, unlabeled polymers were used as the spacing, precoating, and protection layers, while the polymers labeled with P and A were used

[†] Department of Polymer Chemistry.
[‡] Department of Material Chemistry.

S0024-9297(98)00337-4 CCC: $15.00 
Published on Web 08/19/1998

**Chart 1. Chemical Structure of Poly(vinyl alkanal acetal) (PVAA)**

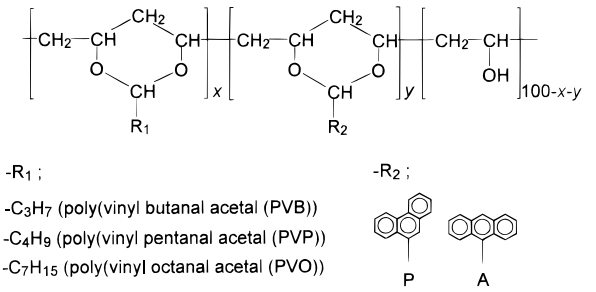


-$R_1$ ;

-$C_3H_7$ (poly(vinyl butanal acetal (PVB))

-$C_4H_9$ (poly(vinyl pentanal acetal (PVP))

-$C_7H_{15}$ (poly(vinyl octanal acetal (PVO))

-$R_2$ ;




**Table 1. Compositions of PVAAs and Surface Pressures at the LB Deposition**

| sample | $x$ (%) | $y$ (%) | $100 - x - y$ (%) | surface pressure (mN m$^{-1}$) |
|---|---|---|---|---|
| PVB | 76 | | 24 | 15 |
| PVB−P | 58 | 7 | 35 | 15 |
| PVB−A | 62 | 2 | 36 | 13 |
| PVP | 66 | | 34 | 20 |
| PVP−P | 65 | 8 | 27 | 18 |
| PVP−A | 62 | 2 | 36 | 18 |
| PVO | 73 | | 27 | 23 |
| PVO−P | 57 | 12 | 31 | 18 |
| PVO−A | 55 | 7 | 38 | 20 |

for the energy-donating layer and -accepting layer, respectively. For the viscoelastic measurement, unlabeled polymers were used. The glass-transition temperatures ($T_g$) of the prepared polymer were measured with a Melter thermosystem model FP-85.

**Preparation of LB Films.** A dilute solution of each polymer (0.1 wt %) in benzene (Dojin, spectrograde) was spread on the pure water in a Teflon-coated trough (Kenkosha model SI-1), and the solvent was allowed to evaporate. Water for the subphase was ion-exchanged, distilled, and passed through a water purification system (Barnstead Nanopure II). The temperature of the subphase was kept at 19 °C for PVO and PVP and at 7 °C for PVB.

The monolayer on the air/water surface was compressed at a rate of 10 mm min$^{-1}$ to an appropriate surface pressure (see Table 1). Then, it was transferred vertically onto a nonfluorescent quartz plate which was cleaned with oxidative sulfuric acid, rinsed with pure water, and then made hydrophobic by dipping into a 10% toluene solution of trimethylchlorosilane for 30 min. The deposition was performed with a good transfer ratio both in the up and down modes, yielding a Y-type LB film.

Figure 1 illustrates the structure of the LB films for the energy-transfer measurements. The sample films were fabricated on a quartz plate in the following sequence: (1) 4 layers of nonchromophoric polymer for the precoating layers, (2) 2 layers of P-labeled polymers for the energy-donating layers, (3) $n$ layers ($n$ = 4, 8) of nonchromophoric polymers for the spacing layers, (4) 2 layers of A-labeled polymers for the energy-accepting layers, and (5) $(10 - n)$ layers of nonchromophoric polymers for the protection layers. Since the total number of layers was kept constant at 18, the samples have the same compositions of three kinds of polymers, regardless of $n$. The thickness of each layer is 0.85 nm for PVB, 0.90 nm for PVP, and 1.02 nm for PVO.[17] These films are abbreviated as PVB-$n$, PVP-$n$, and PVO-$n$, respectively.

**Energy-Transfer Measurements.** Fluorescence spectra of LB films were recorded by a Hitachi 850 fluorescence spectrophotometer equipped with a thermoregulated sample chamber. The temperature was kept constant within ±1 °C. In the measurement of spectral change under the heating and cooling processes, the rates were fixed to be 0.5 °C min$^{-1}$ in the range 25−100 °C. The spectral change under a constant temperature was also measured in the time range of 0−6 h.

Theoretical calculation was performed to examine the disordering process of the layered structure quantitatively. The

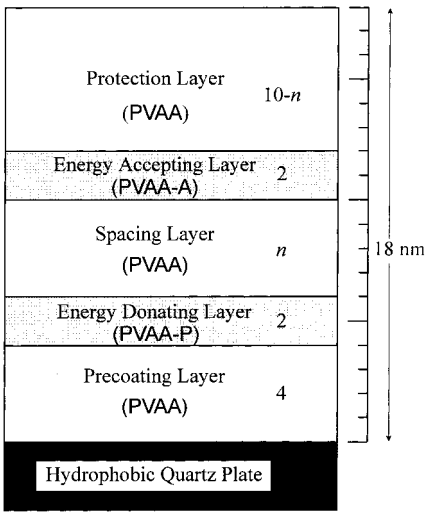


**Figure 1.** Layer structure of LB films for the energy-transfer measurements. The symbol $n$ means the number of the spacing layers, 4 or 8.

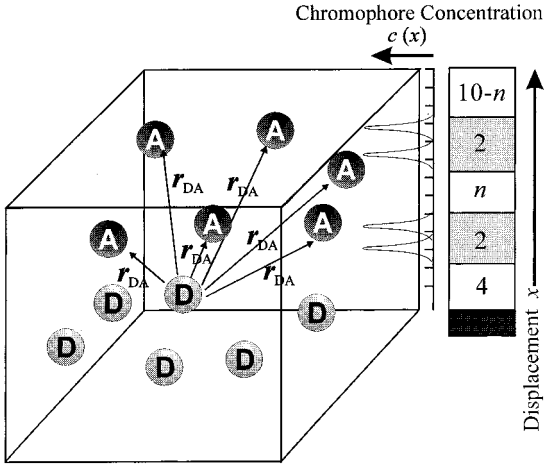


**Figure 2.** Schematic illustration of the model for numerical calculation. D represents phenanthrene chromophore and A represents anthracene chromophore. The distance between the donor and acceptor is denoted by $r_{DA}$.

diffusion constant, $D$, of the polymer chain in the direction of the film thickness was obtained by a method described in detail elsewhere.[14,15] The diffusion in the LB film results in a distribution of chromophores in the direction normal to the film plane. We assumed a Gaussian function for the chromophore distribution, which is characterized by the distribution center $x_0$ and the variance $\sigma^2$:

$$c(x) = \frac{c_0}{\sigma\sqrt{2\pi}} \exp\left(-\frac{(x - x_0)^2}{2\sigma^2}\right) \quad (1)$$

where $c(x)$ is the concentration of chromophores at a displacement $x$ and $c_0$ is related to the total number of chromophores placed in the system. First, donors (D) and acceptors (A) were placed randomly within the lateral direction of each layer, but were kept at a given Gaussian distribution along the $x$ direction; these procedures were performed by a computer using random numbers. The distribution center was positioned to the center of each chromophoric layer. Figure 2 is a schematic illustration of the chromophore distribution in the LB film.

The Förster theory for the energy transfer by the dipole−dipole interaction gives the following rate equation:[17]

$$k_T = \frac{1}{\tau_0}\left(\frac{r_0}{r_{DA}}\right)^6 \quad (2)$$

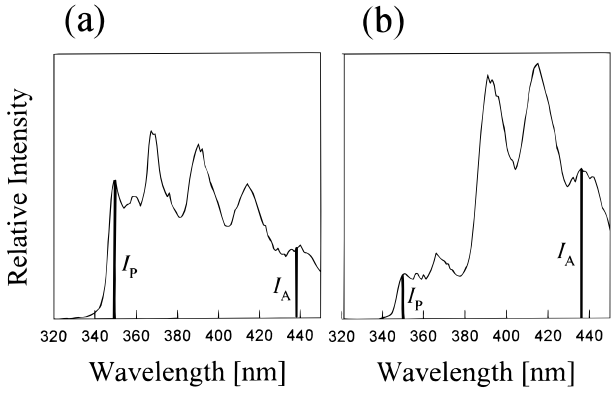


**Figure 3.** Spectral change of PVO-4 films under a constant temperature, 60 °C for 7 h: (a) before heating; (b) after heating. The excitation wavelength is 298 nm.

where $k_T$ is the energy-transfer rate from an excited D to A, $r_{DA}$ is the distance between D and A, $\tau_0$ is the lifetime of D, and $r_0$ is the Förster radius of the D−A pair. These parameters for the phenanthrene and anthracene pair are obtained experimentally as $r_0 = 2.12$ nm and $\tau_0 = 43$ ns.[18] As shown in Figure 2, the distance $r_{DA}$ between all D and A pairs was calculated, and then the energy-transfer efficiency was determined by eq 2 for a given variance $\sigma^2$ of distribution. The variance $\sigma^2$ is a function of time and diffusion constant $D$ as follows:

$$\sigma^2 = 2Dt + {\sigma_0}^2 \tag{3}$$

where ${\sigma_0}^2$ is the initial distribution due to the Y-type deposition of the chromophoric layers and the slight disordering of layers after deposition. Fitting of the theoretical curve to the energy-transfer efficiency plot at a constant temperature allowed us to evaluate $D$.

**Viscoelastic Measurements.** For the viscoelastic measurement, polymers were molded into a disk in a suitable size to fit to the geometry of the rheometer. Dynamic viscoelastic properties were measured using a plate−plate type rheometer (Rheometrics mechanical spectrometer model 605) with a plate diameter of 2.5 cm. The angular frequency ranged from 0.01 to 100 $s^{-1}$, and the strain amplitude was fixed to be 0.1%. The measurements were carried out at several temperatures from the glass-transition region to the flow region.

## Results and Discussion

**Thermal Properties of LB Films Observed by the Energy-Transfer Method.** Figure 3 shows the spectral change of PVO-4 before and after heating. The P chromophores were selectively excited at the wavelength of 298 nm, at which the excitation probability of A was less than 5% of P. But the efficient energy transfer from P to A occurred, yielding both P (at 350 and 367 nm) and A emission (at 393, 416, and 438 nm) on the spectra. Since the energy-transfer rate is proportional to −6th power of the distance between donor and acceptors, one can probe the microscopic changes of the distance in nanometers. As a measure of energy-transfer efficiency, the intensity ratio $I_A/I_P$ was employed, where $I_A$ and $I_P$ are the intensity of A emission at 438 nm and the intensity of P emission at 350 nm, respectively. A trace amount of P emission at 438 nm was subtracted from the $I_A$ actually observed. The use of $I_A/I_P$ enables convenient evaluation of the energy-transfer efficiency, without consideration of errors among samples on the measurement of relative intensities.

As Figure 3 shows, thermal treatment changed the spectra markedly; the $I_A$ increased and the $I_P$ decreased,

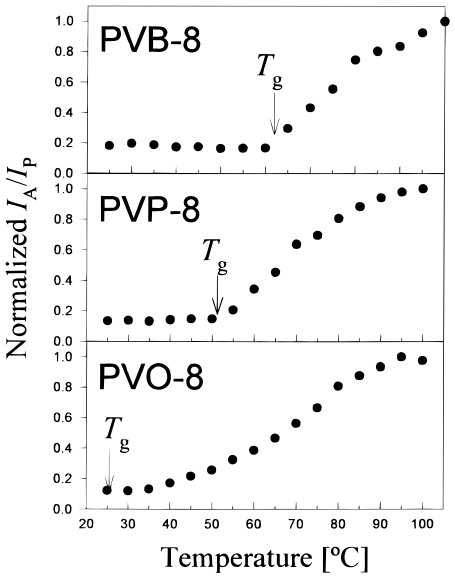


**Figure 4.** Effect of heating on the energy-transfer efficiency for PVAA LB films. The rate of heating was fixed to 0.5 °C $min^{-1}$.

**Table 2. Thickness of Spacing Layers, Critical Temperatures ($T_c$) of LB Films, and Glass-Transition Temperatures ($T_g$) of Bulk Polymers**

| sample | thickness (nm) | $T_c$ (°C) | $T_g$ (°C) |
|---|---|---|---|
| PVB-8 | 6.8 | 60 | 63 |
| PVP-8 | 7.2 | 50 | 51 |
| PVO-8 | 8.2 | 35 | 25 |

resulting in the increase of $I_A/I_P$. After the sample was heated to about 100 °C, further appreciable change was not seen with the subsequent thermal treatments. The thermal treatment gave rise to considerable change of $I_A/I_P$ but no appreciable wavelength shift on both absorption and fluorescence spectra. This indicates that the layered structure is irreversibly disordered and all layers are totally mixed by the heating process. P and A chromophores separated at the beginning become closer by the structural relaxation, and the decrease of $r_{DA}$ on average yields the increase of energy-transfer efficiency. The values of $I_A/I_P$ after the sufficient thermal treatment were almost the same as the calculated values of the transfer efficiency under the condition of a uniform dispersion of P and A chromophores. This means that in the equilibrium state after the relaxation each layer was mixed and P and A chromophores were randomized in the film.

Figure 4 shows the plots of $I_A/I_P$ on the first course of heating for PVB-8, PVP-8, and PVO-8. The ratio is normalized by the maximum value to compensate for the difference in acceptor concentration among samples. Initially, the chromophoric layers were separated by eight layers of spacing polymer, the thickness of which is given in Table 2. The energy-transfer efficiency markedly increased with heating, revealing that the P and A chromophores become closer than the initial location, as described before. Table 2 also shows glass-transition temperatures of the bulk polymer $T_g$, and the critical temperatures $T_c$, at which the rapid increase of the energy-transfer efficiency starts. These temperatures depended on the length of the polymer side chains. The longer the side chain, the lower the value of $T_g$ due to the flexibility of alkyl chains. This again affects the rate of disordering of the LB films and indicates a close relationship between $T_g$ and $T_c$. It is natural to assume

that the polymer chains have similar flexibility and mobility both in a polymer bulk and in an ultrathin film. The glass transition is attributed to a micro-Brownian motion of the polymer main chain. At a specific temperature a polymer main chain starts to change its conformation within a free volume of polymer bulk, which is closely related to the degree of packing of the polymer side chains.

Hsiung et al. investigated the orientational disordering of the side chain in polymer LB films by the optical SHG method.[10] They reported that the transition range in LB films is similar to the range of bulk glass transition, which is consistent with our result. In both cases, the disordering transition is dominated by the intrinsic relaxation of the polymer main chain. From these results it is concluded that the relaxation process is closely related to the bulk properties of LB materials. However, the mode of polymer chain motions in the layered structure of LB films must be different from those of the 3D bulk state. We will examine the relaxation behavior more quantitatively with respect to activation energies.

**Evaluation of Activation Energy in LB Films.** The fluorescence method, which gives effective information not only about the distance of chromophores but also about the distribution of the distance,[14] was applied to the relaxation process in the polymer LB films of PVB-4, PVP-4, and PVO-4; each thickness of spacing layers was approximately 4 nm. A small number of chromophores were introduced into the polymer as a side chain, to obtain the uniform dispersion of chromophores in a layer plane.[5b] Thus, the diffusion of chromophores can be regarded as that of polymer chains. In the present system, we assumed a Gaussian distribution along the direction normal to the layer plane, since a Gaussian distribution seems to be a reasonable expression on the course of the diffusion process. Diffusion constant $D$ represents the structural relaxation rate of multilayer structure. Obtained values of $D$ in eq 3 are in the order of $10^{-15}-10^{-18}$ cm$^2$ s$^{-1}$ (plotted against $1000/T$ in Figure 5), being similar to the values reported for the diffusion phenomenon in the rubbery state of polymer bulk: the diffusion at the polymer−polymer interface[19−21] or the diffusion in polymer blends.[22] This result also shows the similarity of thermal properties between the LB film and the bulk. The apparent activation energy for the polymer diffusion, $\Delta E_{aLB}$, was evaluated by Ahhrenius plots over a limited temperatures range:

$$D = D_0 \exp\left(-\frac{\Delta E_{aLB}}{RT}\right) \tag{4}$$

The values of $\Delta E_{aLB}$ obtained are listed in Table 3. It should be noted that these values are much smaller than the values of apparent activation energy observed for polymer bulk, as described in the later section.

**Evaluation of Activation Energy in Bulk Polymers.** The dynamic viscoelastic measurement is a useful method to analyze relaxation processes of the polymer bulk, polymer melt, and condensed polymer solution. According to the empirical principle of time−temperature superposition,[23] the frequency dependence of complex modulus $G^*(\omega,T)$ at two temperatures shows by a simple scale change

$$G^*(\omega,T) = b_T G^*(a_T\omega,T_0) \tag{5}$$

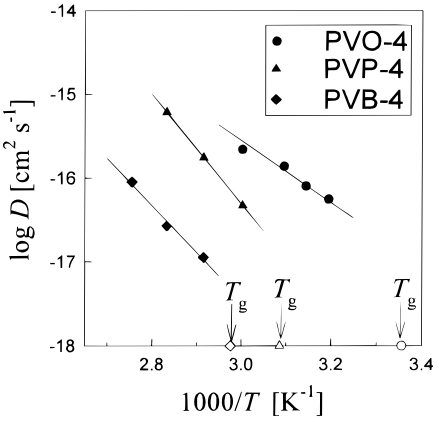


**Figure 5.** Diffusion constant $D$ plotted against $1000/T$: (◆) PVB; (▲) PVP; (●) PVO. Open symbol denotes $T_g$: (◇) PVB; (△) PVP; (○) PVO.

**Table 3. Apparent Activation Energies Measured by the Energy-Transfer Method ($\Delta E_{aLB}$) and by the Viscoelastic Measurement ($\Delta E_{aBULK}$)**

| sample | $\Delta E_{aLB}$ (kJ/mol) | $\Delta E_{aBULK}$ (kJ/mol)[a] | temperature range (°C)[b] |
|---|---|---|---|
| PVB | 110 | 220 | 70−90 |
| PVP | 120 | 240 | 60−80 |
| PVO | 70 | 180 | 40−60 |

[a] The value at $T_g$ + 20 °C. [b] Range of the energy-transfer measurements for LB films (see Figure 8).

This principle was found to be valid for the bulk PVAA system and utilized to make a master curve. The adjustable parameters, $a_T$ and $b_T$, are functions of temperature, but not of frequency. The effect of the modulus scale shift was found to be very small and $b_T$ could be regarded as unity here. Figure 6a shows the storage modulus $G'$ and the loss modulus $G''$ plotted against angular frequency $\omega$ for PVO at various temperatures from 25 to 102 °C. The frequency dependence of $G'$ and $G''$ can be superimposed onto the master curve by a horizontal shift along the frequency axis. Figure 6b shows the master curves of $G'$ and $G''$ at the reference temperature of 53 °C. $G'$ and $G''$ can be superposed successfully by a common shift factor $a_T$. However, strictly speaking, $G'$ curves measured at a higher temperature came to a little higher position than $G'$ curves measured at a lower temperature. This is probably due to thermal-cross-linking of hydroxyl groups in the polymer chain, which gives rigidity.

The master curves represent the frequency dependence at a constant temperature, which can cover a wide temperature range. The shift factor $a_T$ employed for the time-temperature superposition follows the WLF equation:[24]

$$\log a_T = \frac{C_1(T - T_0)}{C_2 + T - T_0} \tag{6}$$

where $C_1$ and $C_2$ are constants and $T_0$ is a reference temperature. As shown in Figure 7, the plot of $-(T - T_0)/\log a_T$ versus $T - T_0$ gave straight lines. The values of $C_1$ and $C_2$ can be calculated from the slope $s$ and the intercept $i$ of these lines as $C_1 = 1/s$ and $C_2 = i/s$. Table 4 shows the values of $C_1$ and $C_2$ determined by this method.

The temperature dependence of the shift factor yields an Arrhenius form, with a linear dependence of $\log a_T$ on $1/RT$. The slope $\Delta E_{aBULK}$ is interpreted as an

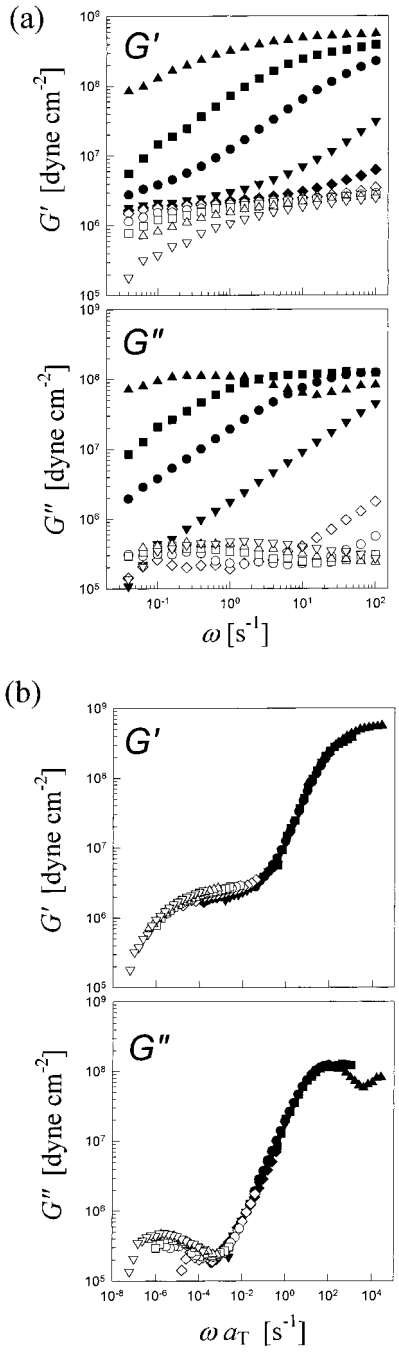


**Figure 6.** (a) Storage modulus $G'$ and loss modulus $G''$ plotted against angular frequency $\omega$ at various temperatures. (b) Master curves of $G'$ and $G''$ for PVO: at (▲) 15 °C; (■) 20 °C; (●) 25 °C; (▼) 35 °C; (◆) 43 °C; (◇) 55 °C; (○) 66 °C; (□) 76 °C; (△) 86 °C; (▽) 102 °C. The reference temperature $T_0$ is 53 °C.

apparent activation energy for viscoelastic relaxation. From eq 6, $\Delta E_{aBULK}$ can be calculated formally as a function of temperature as follows:

$$\Delta E_{aBULK} = R\frac{d(\ln a_T)}{d(1/T)} = 2.303R\frac{C_1C_2T^2}{(C_2 + T - T_0)^2} \quad (7)$$

Figure 8 shows the temperature dependence of $\Delta E_{aBULK}$ obtained from eq 7. The solid part of each line shows the range in which the energy-transfer measurements for LB films were performed, and $T_g$ of each sample is also depicted in the figure. As the representative value of the apparent activation energy for the

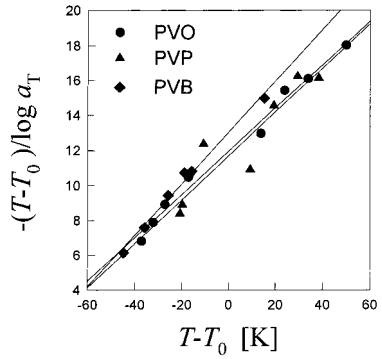


**Figure 7.** $-(T - T_0)/\log a_T$ plotted against $T - T_0$: (◆) PVB; (▲) PVP; (●) PVO. The values of reference temperature $T_0$ are shown in Table 3.

**Table 4. WLF Parameters for the Bulk PVAAs**

| sample | $C_1$ | $C_2$ | $T_0$ (°C) |
|---|---|---|---|
| PVB | 7.64 | 94.2 | 91 |
| PVP | 8.39 | 101 | 85 |
| PVO | 8.45 | 101 | 53 |

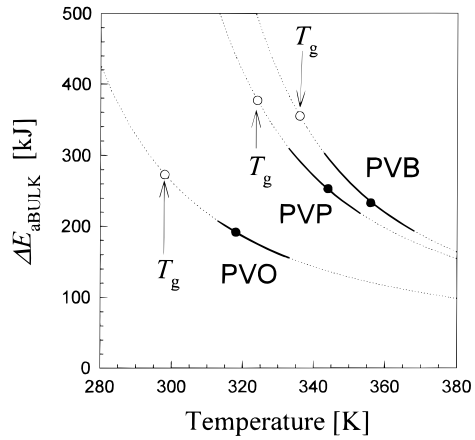


**Figure 8.** Temperature dependence of apparent activation energy $\Delta E_{aBULK}$ for PVAAs calculated from eq 7. Open circle on each curve shows the glass-transition temperature of each polymer. Filled circle shows $T_g$ + 20 °C.

bulk, $\Delta E_{aBULK}$ at the temperature of $T_g$ + 20 °C is employed because the temperature is almost in the middle of the range where the energy-transfer measurements for the LB films were performed (see filled circles in Figure 7). Now we are able to compare $\Delta E_{aBULK}(T_g + 20\ °C)$ with $\Delta E_{aLB}$ in the same temperature range; Table 3 shows the values obtained. The relative order of these values was consistent each other, indicating the close relation of thermal properties of LB and bulk systems, as previously seen in the measurements of $T_c$.

**Comparison of Apparent Activation Energies: Characteristics in Polymer Ultrathin Films.** The most important fact is that the values of $\Delta E_{aLB}$ are much smaller than those of $\Delta E_{aBULK}$. This significant difference in the activation energies between the LB films and the bulk is probably attributed to the difference of modes of molecular motion contributing to each relaxation process.

Herein, we should examine the following two points. *First*, the scale of the relaxation observed in LB films is as small as several nanometers. Assuming that one polymeric chain takes a circular form on the water surface, its radius is calculated to be approximately 9 nm from the limiting area of the $\Pi-A$ curve and the molecular weight. Since a real chain is interpenetrated

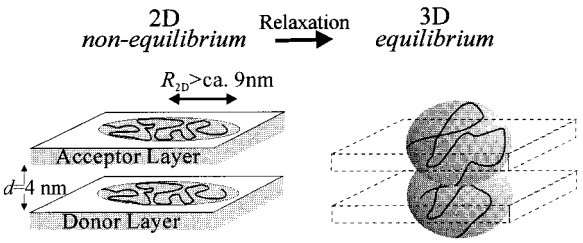


**Figure 9.** Schematic illustration of the structural relaxation of polymer LB films. Here, the chromophoric layers are separated by four spacing layers. Thickness of the single layer for PVAA is approximately 1 nm; thus, the distance between donor and acceptor layers is approximately 4 nm.

with neighboring chains, the actual radius could be larger than 9 nm, which is much greater than the thickness of spacing layers, approximately 4 nm. A schematic view of a single chain in the LB film is illustrated in Figure 9. Thus, a large scale of molecular motion such as translational displacement of the whole chain is not required to disorder the layered structure; a short-range motion of polymer segments would be sufficient. *Second*, the conformational rearrangement of the polymer chain from the nonequilibrium state plays an important role in the relaxation, that is, "*entropy relaxation*". In the course of the preparation of LB films, a monolayer is formed from a dilute solution of the polymer on the water surface; therefore, an individual polymer chain, being isolated, is confined to the 2D plane. By successive compression, the polymer chains are packed and interpenetrated while keeping the 2D conformation. This conformation is transferred on a substrate by deposition. However, once deposited onto a substrate from the air/water interface, the polymer chain is free from the restriction to keep a 2D conformation (see Figure 9). Therefore, the relaxation of a polymer chain in ultrathin films is considered to proceed with a smaller activation energy than an equilibrium chain in the polymer bulk.

## Conclusion

The thermal relaxation of polymer LB films was measured by the energy-transfer method. The relaxation properties of LB films have a close relation to those of bulk polymers, but gave much smaller apparent activation energy than the bulk systems. Disordering of the layered structure is mainly governed by the local motion of polymer segments, and conformational rearrangement occurs from the nonequilibrium state confined to a 2D plane, which seems to be a characteristic of the relaxation of polymer LB films.

The result means that even a local motion of polymer segments causes a fatal damage to the layered structure. Therefore, for the stabilization of the multilayered structure of ultrathin the polymer films, it is important to take a progressive measure to fix the segmental motion of polymer chain. Several approaches have been taken to obtain thermally stable polymer LB films such as cross-linking of polymer chains after the deposition,[13,24,25] preparation of polymers with a rigid main chain,[26−29] and a self-organizing side chain.[8]

**Acknowledgment.** The authors thank Mr. Nobuyuki Hori for the technical assistance of the viscoelastic measurements. The present study was supported by a Grant-in-Aid for Science Research (No. 09450360) from the Ministry of Education, Science, Sports, and Culture of Japan. S. Ito acknowledges the Sumitomo Foundation for financial support.

## References and Notes

(1) Ulman, A. *An Introduction of Ultrathin Organic Films from Langmuir−Blodgett to Self-Assembly*; Academic Press: San Diego, CA, 1991; Part 2.
(2) Kuhn, H.; Möbius, D.; Bücher, H. *Physical Methods of Chemistry*; Weissberger, A., Rossiter, B. W., Eds.; Wiley: New York, 1972; p 557, Vol. 1, Part 3B.
(3) (a) Tredgold, R. H.; Winter, C. S. *J. Phys. D, Appl. Phys.* **1982**, *15*, L55. (b) Tredgold, R. H.; Winter, C. S. *Thin Solid Films* **1983**, *99*, 81. (c) Tredgold, R. H. *Thin Solid Films* **1987**, *152*, 223.
(4) (a) Watanabe, M.; Kosaka, Y.; Oguchi, K.; Sanui, K.; Ogata, N. *Macromolecules* **1988**, *21*, 2997. (b) Oguchi, K.; Yoden, T.; Kosaka, Y.; Watanabe, M.; Sanui, K.; Ogata, N. *Thin Solid Films* **1988**, *161*, 305.
(5) (a) Ito, S.; Okubo, H.; Ohmori, S.; Yamamoto, M. *Thin Solid Films* **1989**, *179*, 445. (b) Ohmori, S.; Ito, S.; Yamamoto, M.; Yonezawa, Y.; Hada, H. *J. Chem. Soc., Chem. Commun.* **1989**, 1293.
(6) Ringsdorf. H.; Schmidt, G.; Schneider, J. *Thin Solid Films* **1987**, *152*, 207.
(7) Biddle, M. B.; Lando, J. B.; Ringsdorf, H.; Schmidt, G.; Schneider, J. *Colloid Polym. Sci.* **1988**, *266*, 806.
(8) Schneider, J.; Ringsdorf, H.; Rabolt, J. F. *Macromolecules* **1989**, *22*, 205.
(9) Schneider, J.; Erdelen, C.; Ringsdorf, H.; Rabolt, J. F. *Macromolecules* **1989**, *22*, 3475.
(10) Hsiung, H.; Beckbauer, R.; Rodriguez-Parada, J. M. *Langmuir* **1993**, *9*, 1971.
(11) Ohmori, S.; Ito, S.; Yamamoto, M. *Macromolecules* **1991**, *24*, 2377.
(12) Ueno, T.; Ito, S.; Ohmori, S.; Onogi, Y.; Yamamoto, M. *Macromolecules* **1992**, *25*, 7150.
(13) Ito, S.; Ueno, T.; Yamamoto, M. *Thin Solid Films* **1992**, *210/211*, 614.
(14) Hayashi, T.; Okuyama, T.; Ito, S.; Yamamoto, M. *Macromolecules* **1994**, *27*, 2270.
(15) Yamamoto, M.; Kawano, K.; Okuyama, T.; Hayashi T.; Ito, S. *Proc. Jpn. Acad.* **1994**, *70(B)*, 121.
(16) Ito, S.; Kawano, K.; Hayashi, T.; Yamamoto, M. *Polym. J.* **1996**, *28*, 164.
(17) Förster, Th. *Z. Naturforsch., A: Phys. Sci.* **1949**, *4*, 321.
(18) Berlman, I. B. *Energy Transfer Parameters of Aromatic Compounds*; Academic Press: New York, 1973.
(19) (a) Zhao, C.; Wang, Y.; Hruska, Z.; Winnik, M. A. *Macromolecules* **1990**, *23*, 4082. (b) Wang, Y.; Winnik, M. A. *J. Chem. Phys.* **1991**, *95*, 2143. (c) Wang, Y.; Winnik, M. A. *Macromolecules* **1993**, *26*, 3147. (d) Pekcan, Ö.; Winnik, M. A.; Croucher, M. D. *Macromolecules* **1990**, *23*, 2673.
(20) Deppe, D. D.; Dhinojwaka, A.; Torkelson, J. M. *Macromolecules* **1996**, *29*, 3898.
(21) Yukioka, S.; Nagato, K.; Inoue, T. *Polymer* **1992**, *33*, 1171.
(22) Nealey, P. F.; Cohen, R. E.; Argen, A. S.; *Macromolecules* **1993**, *26*, 1287.
(23) Ferry. J. D. *Viscoelastic Properties of Polymers*, 3rd ed.; Wiley: New York, 1980; Chapter 11.
(24) Hayashi, T.; Mabuchi, M.; Mitsuishi, M.; Ito, S.; Yamamoto, M.; Knoll, W. *Macromolecules* **1995**, *28*, 2537.
(25) Aoki, A.; Nakaya, M.; Miyashita, T. *Chem. Lett.* **1996**, 667.
(26) (a) Duda, G.; Schouten, A. J.; Arndt, T.; Lieser, G.; Schmidt, G. F.; Bubeck, C.; Wegner, G. *Thin Solid Films* **1988**, *159*, 221. (b) Orthmann, E.; Wegner, G. *Makromol. Chem., Rapid Commun.* **1986**, *7*, 243. (c) Orthmann, E.; Wegner, G. *Angew. Chem., Int. Ed. Engl.* **1986**, *25*, 1105.
(27) Embs, F.; Funhoff, D.; Laschewski, A.; Licht, U.; Ohst, H.; Prass, W.; Ringsdorf, H.; Wegner, G.; Wehrmann, R. *Adv. Mater.* **1991**, *3*, 25.
(28) Sauer, T.; Arndt, T.; Batchelder, D. N.; Kalachev, A. A.; Wegner, G. *Thin Solid Films* **1990**, *187*, 357.
(29) Kakimoto, M.; Suzuki, M.; Konishi, T.; Imai, Y.; Iwamoto, M.; Hino, T. *Chem. Lett.* **1986**, 823.

MA980337+